LLNL-CONF-415387

LAWRENCE
LIVERMORE
NATIONAL
LABORATORY

Avoiding the False Peaks in Correlation Discrimination

A. A. S. Awwal

August 6, 2009

SPIE Optics & Photonics
San Diego, CA, United States
August 2, 2009 through August 6, 2009

Avoiding the false peaks in correlation discrimination

Abdul A. S. Awwal

Laser Science Engineering and Operations, National Ignition Facility

Lawrence Livermore National Laboratory, Livermore, CA. 94551

E-mail: awwal1@llnl.gov

ABSTRACT

Fiducials imprinted on laser beams are used to perform video image based alignment of the 192 laser beams in the National Ignition Facility (NIF) of Lawrence Livermore National Laboratory. In many video images, matched filtering is used to detect the location of these fiducials. Generally, the highest correlation peak is used to determine the position of the fiducials. However, when the signal to-be-detected is very weak compared to the noise, this approach totally breaks down. The highest peaks act as traps for false detection. The active target images used for automatic alignment in the National Ignition Facility are examples of such images. In these images, the fiducials of interest exhibit extremely low intensity and contrast, surrounded by high intensity reflection from metallic objects. Consequently, the highest correlation peaks are caused by these bright objects. In this work, we show how the shape of the correlation is exploited to isolate the valid matches from hundreds of invalid correlation peaks, and therefore identify extremely faint fiducials under very challenging imaging conditions.

Key word: Pattern recognition, image processing, correlation shape, laser alignment

1. INTRODUCTION

The National Ignition Facility (NIF), developed at the Lawrence Livermore National Laboratory, is a stadium-sized facility that contains a 192-beam, 1.8-megajoule, 500-terawatt, ultraviolet laser system dedicated to the study of inertial confinement fusion and the physics of matter at extreme energy densities and pressures [1]. The alignment of this high energy pulsed laser is a critical process requiring high accuracy error-free measurement [2-4]. If the beam alignment is not performed accurately the objective of producing high energy density and pressure cannot be fulfilled.
An automatic alignment (AA) system was designed and implemented to ensure successful delivery of high energy pulse in each of the 192 beams.

Alignment of the laser beams is performed by an automated control system which controls more than 12,000. Each beam is aligned by knowing the current position of the beam, and controlling mirrors and other devices to bring the beam to a desired reference location. The position of the beam is determined by algorithms processing beam images with or without any fiducials. Numerous types of images are being processed throughout the beam path of each laser beam. When there are no definite fiducials, such as in the case of small-width Gaussian laser beams, centroiding is the preferred method for finding the beam position. However, when the beam is represented by a fiducial, matched filtering is the preferred method to detect the location of these fiducials [5-11]. The advantage of the matched filtering is low susceptibility to noise, invariance to local intensity variation resulting in higher temporal stability of beam position, adaptability to various types and sizes of the fiducials etc.

Generally, in matched filtering the position of the highest correlation peak indicates the position of the fiducials. However, when the signal strength of the fiducial is very weak compared to the noise, this assumption of maximum correlation peak appearing at the fiducial position becomes totally invalid. Rather, the highest peaks act as traps for false detection. The active target images used for automatic alignment in the National Ignition Facility are examples of such images. In these images, the fiducials of interest are of extremely low intensity and contrast, surrounded by high intensity reflection from metallic objects. Consequently, the highest correlation peaks are generated by these bright objects which leads to many false correlation peaks. In this work, we demonstrate how the shape of the autocorrelation is exploited to isolate the valid matches from hundreds of false matches.

2. BACKGROUND

The detection algorithm utilized here is based on classical matched filter (CMF). A CMF [12] can be defined by assuming that the Fourier transform of the object function $f(x,y)$ be denoted by:

$$F(U_x,U_y) = \left|F(U_x,U_y)\right| \exp(j\Phi(U_x,U_y)) \tag{1}$$

Then the CMF corresponding to this function $f(x,y)$, given by the complex conjugate of the input Fourier spectrum as denoted by Eq. 2,

$$H_{CMF}(U_x,U_y) = F^*(U_x,U_y) = \left|F(U_x,U_y)\right| \exp(-j\Phi(U_x,U_y)) \tag{2}$$

is expected to produce its autocorrelation. The performance of the matched filter can be further enhanced by performing edge detection on the image and using the edge of the to-be-detected features as the filter. This has an equivalent effect of high pass filtering the correlation plane output, thus increasing the sharpness of the peaks [13-15].

The position of the object can be found from the position of the cross correlation, autocorrelation, and the position of the template using the Eqs. 6-7.

$$x_{pos} = x_{cross} - x_{auto} + x_c \tag{6}$$

$$y_{pos} = y_{cross} - y_{auto} + y_c \tag{7}$$

where (x_{pos},y_{pos}) is the to-be-determined position of the pattern in the image plane, (x_{auto},y_{auto}) is the position of the template autocorrelation peaks and (x_{cross},y_{cross}) is the position of the cross correlation peak. The position of the cross-correlation peak was estimated using a polynomial fit of second order to the correlation peak. The center of the template, (x_c,y_c), and (x_{auto},y_{auto}) is calculated off-line. By centering the template to the center of the image, (x_c,y_c) and (x_{auto},y_{auto}) cancel each-other.

3. ALGORITHM FOR DETECTING FAINT BEAM FIDUCIALS

The active target image depicted in Fig. 1 consists of an image of a CCD array, where the fiducials are etched into the CCD. Note that here the objective is to determine the position of the camera itself, before using the camera to find the position of the beam at the target chamber center. Thus these fiducials represent the position of the camera. Two different views of this CCD array are captured by two different cameras: the first view is taken by a camera along the normal to the surface, the other at a 15 degree angle to the surface. In the normal view, the faint fiducials are shown as flat elliptical objects as shown in Fig. 1(a). In the second view as shown in Fig. 1(b), the same fiducials now appear to be much smaller. The noise is amplified by higher reflection from the metallic electrical connections around CCD chip, while the fiducial loses its contrast due to small angle of observance. In both of these imaging conditions, the fiducials of interest are of extremely low intensity and contrast with very bright noise in the background.

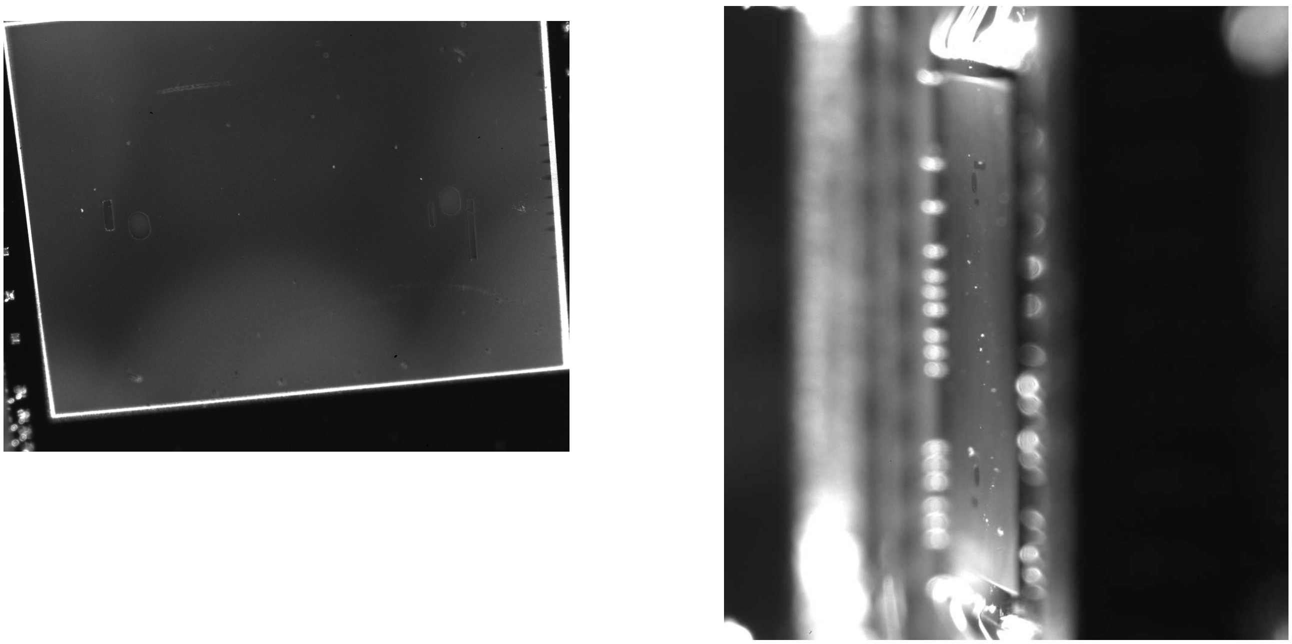

(a) (b)

Fig. 1: Two active target images showing the fiducials to-be-detected, which are barely visible with extremely low contrast. (a) The left image shows the top view of the CCD array. (b) The image on the right, known as side camera image, shows the presence of extremely bright noise source.

One of the prerequisites of using a matched filter is the existence of a template that faithfully represents the to-be-detected pattern. The first step of the active target image processing algorithm is to determine the appropriate template corresponding to the elliptically shaped fiducial. A template is formed by selecting a fiducial from one of the real images as shown in Fig. 2(b). To increase the detection performance, edge detection and careful filtering of the template is performed to create an edge image of the fiducial. The whole image is searched utilizing this template to find the occurrence of the elliptic fiducial.

When correlated with the image in Fig. 2(a), the resulting correlation plane output is shown in Fig. 2(c) shows a large number of peaks corresponding to many false matches.

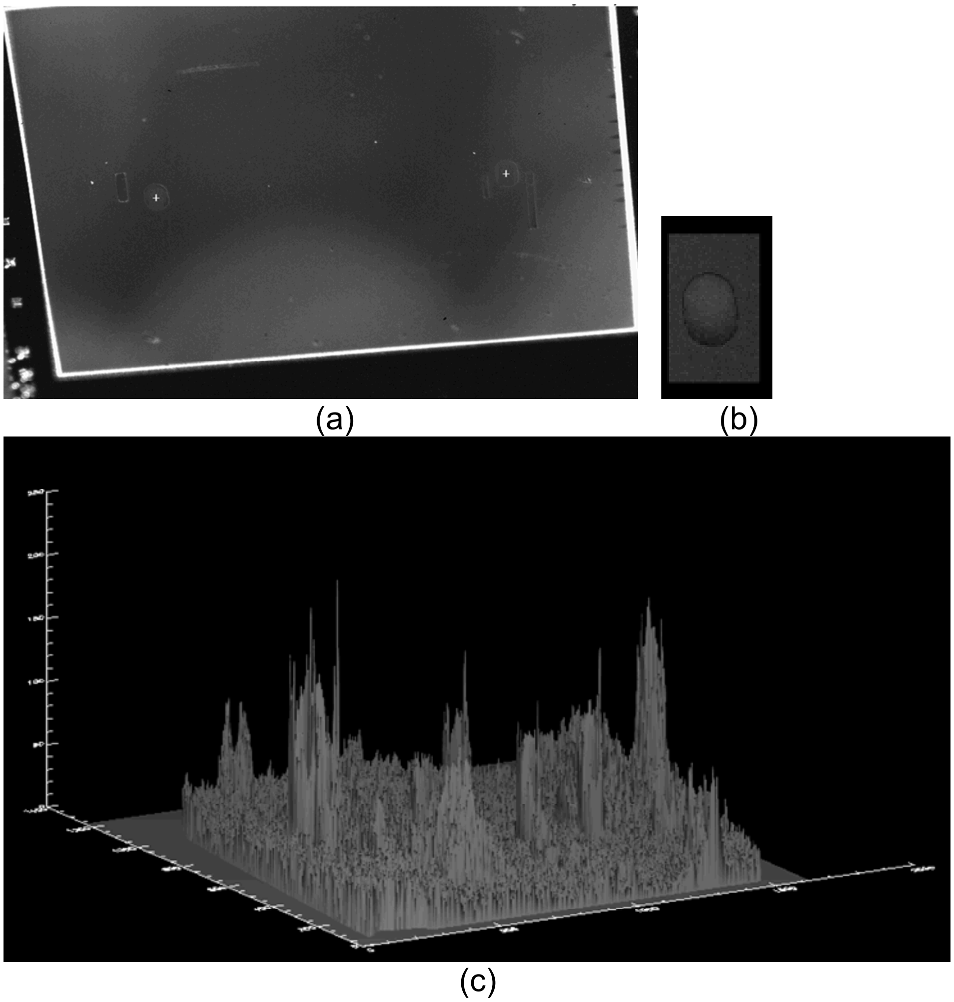

Fig. 2: (a) Active target images showing the fiducials to-be-detected, which are barely visible with extremely low contrast. A side view of this image at an angle of nearly 15 degrees, is shown later in Fig. 4 (a). (b) Template chosen from a real image. (c) Correlation plane output displaying a large number of peaks of which only two are valid.

Note that we removed the bright lines in the preprocessing stage to minimize false correlations. To separate the false peaks from the real peaks, first the autocorrelation is generated from the template, which is shown in Fig. 3(a). Then a segment is cut around the autocorrelation peak and used as a template for difference comparison as shown in Fig. 3(b). It is compared to the first peak in Fig. 3(c). Since the difference is smaller than a specified threshold, it is accepted. The next two peaks as shown in Fig. 3(d-e) turn out to be false peaks. Finally the second peak is detected as shown in Fig. 3(f). In case the processing steps do not remove all the brighter noise, as many as 30 false peaks may have to be discarded before finding all the real peaks.

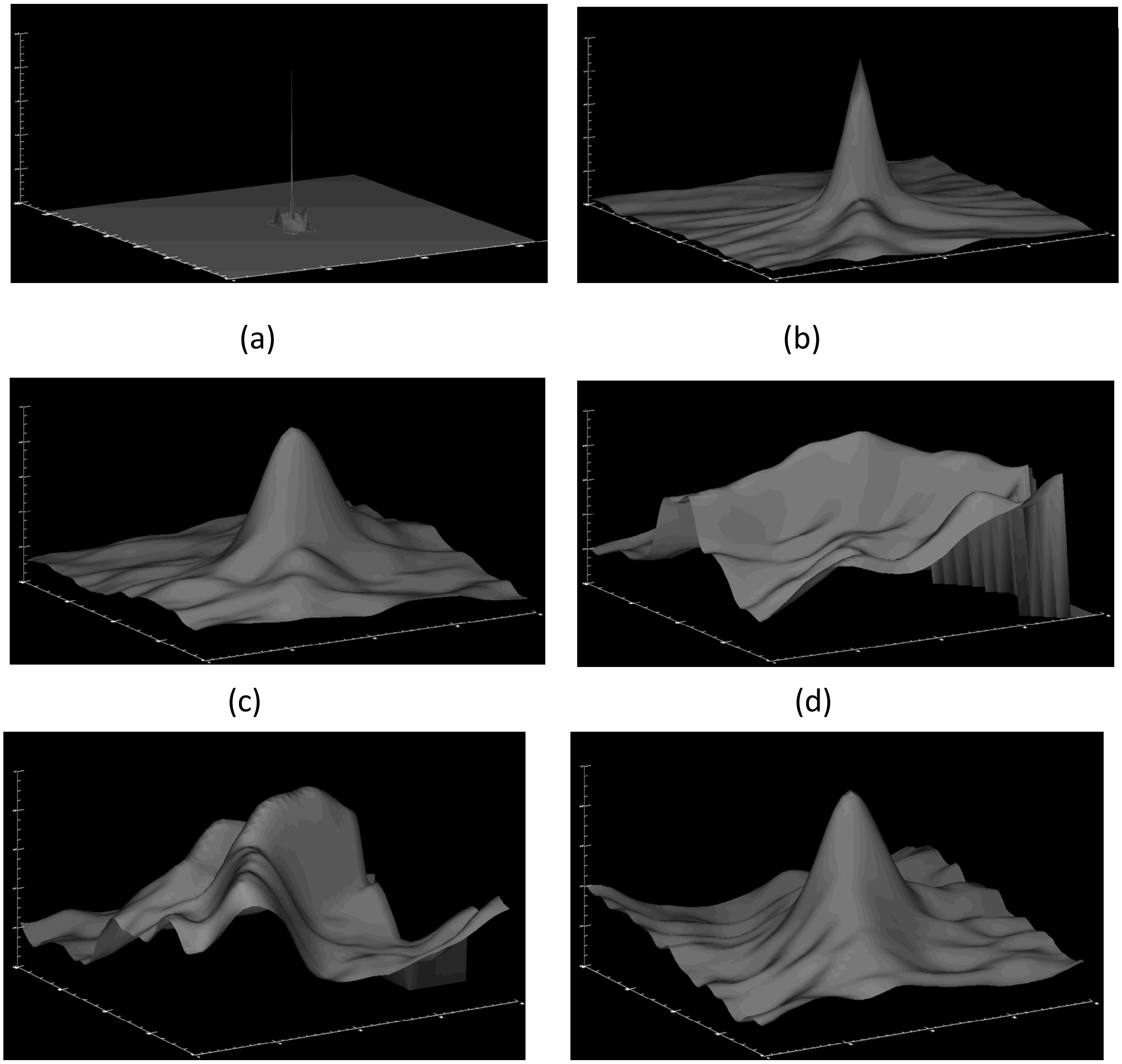

(a) (b) (c) (d) (e) (f)

Fig. 3: (a) Total autocorrelation plane. (b) Segmented autocorrelation. (c) First detected maxima from the cross-correlation plane, matches with autocorrelation. (d) Second maxima does not match. (e) Third maxima does not match. (f) Fourth maxima matches with the self-correlation and is selected.

The active target side images depicted in Fig. 4(a) present the most difficult challenge. Note that when a template generated from real image is used as a matched filter, a huge number of false peaks appear in the correlation plane as shown in Fig. 4(b). Also the challenge is exacerbated by the fact that the contrast of the target is very low and in the presence of many high contrast features of various sizes in the image. Moreover, many parts of the image have very similar features such as the faint fiducials. The highest correlation peaks are generated by the bright noise sources. To enhance the correlation performance, filtered edge images generated from the real images are used as template.

The segmented autocorrelation is shown in Fig. 5(a). In the case of side image in Fig. 4(a) however, the difference criteria did not provide sufficient discrimination. The true match was identified using the standard deviation of the product of the inverse. In some images, the true peaks may be identified after 90 or more correlation comparisons. The shape of the correlation is exploited to filter out a valid match from as many as hundreds of invalid matches. Using the information from self-correlation, we are able to avoid false matches and find the best match under very challenging lighting conditions.

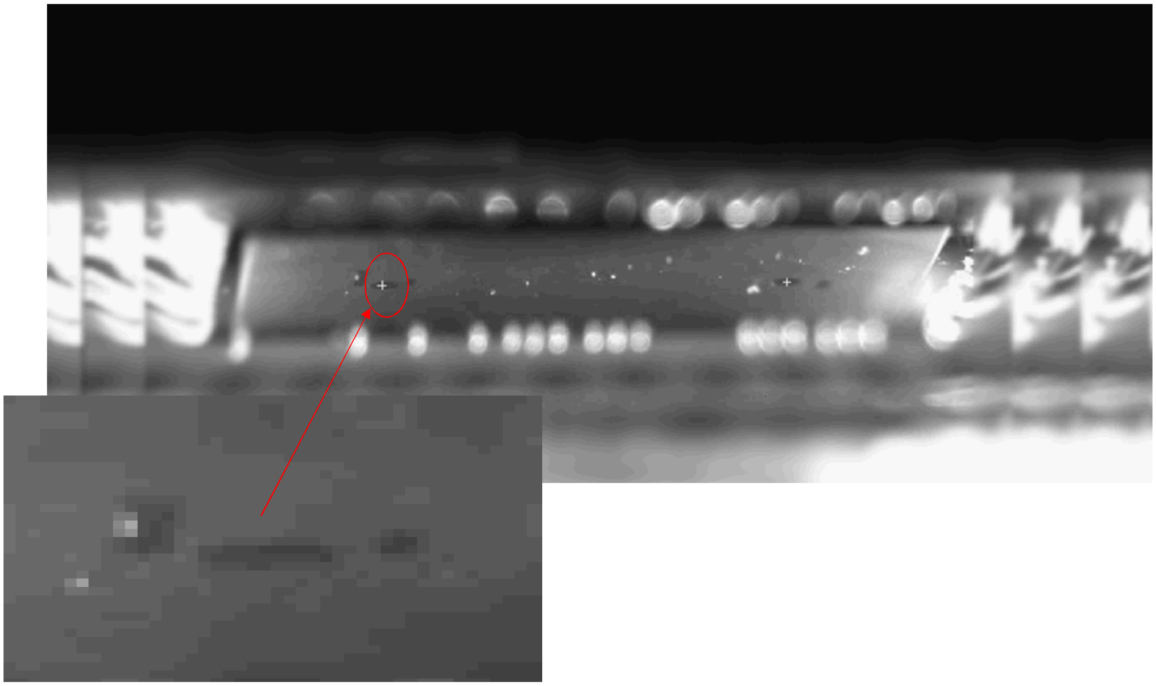

(a)

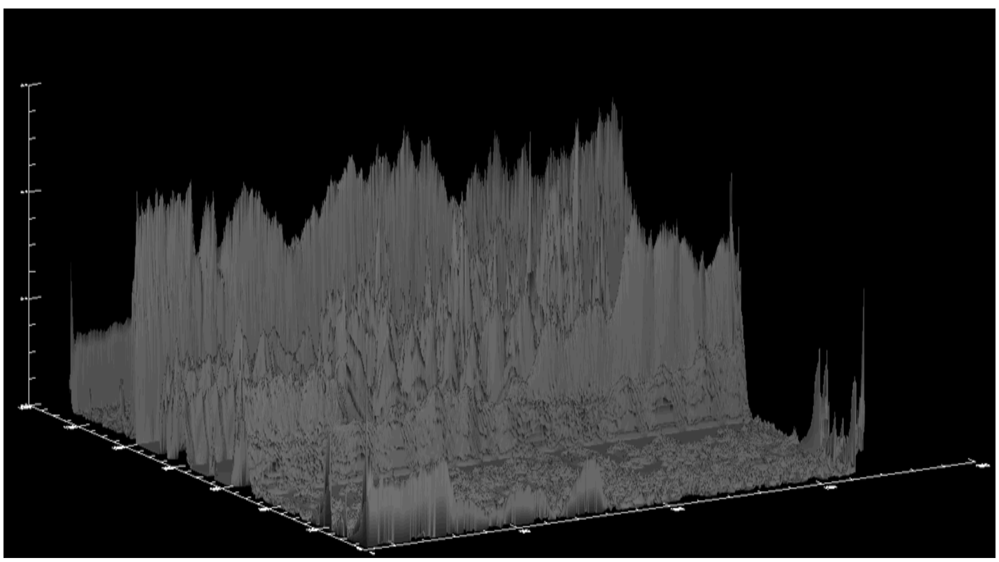

(b)

Fig. 4: (a) Active target side images showing extremely low contrast fiducials with very high brightness noise. (b) The correlation plane output shows a large number of peaks due to high noise count.

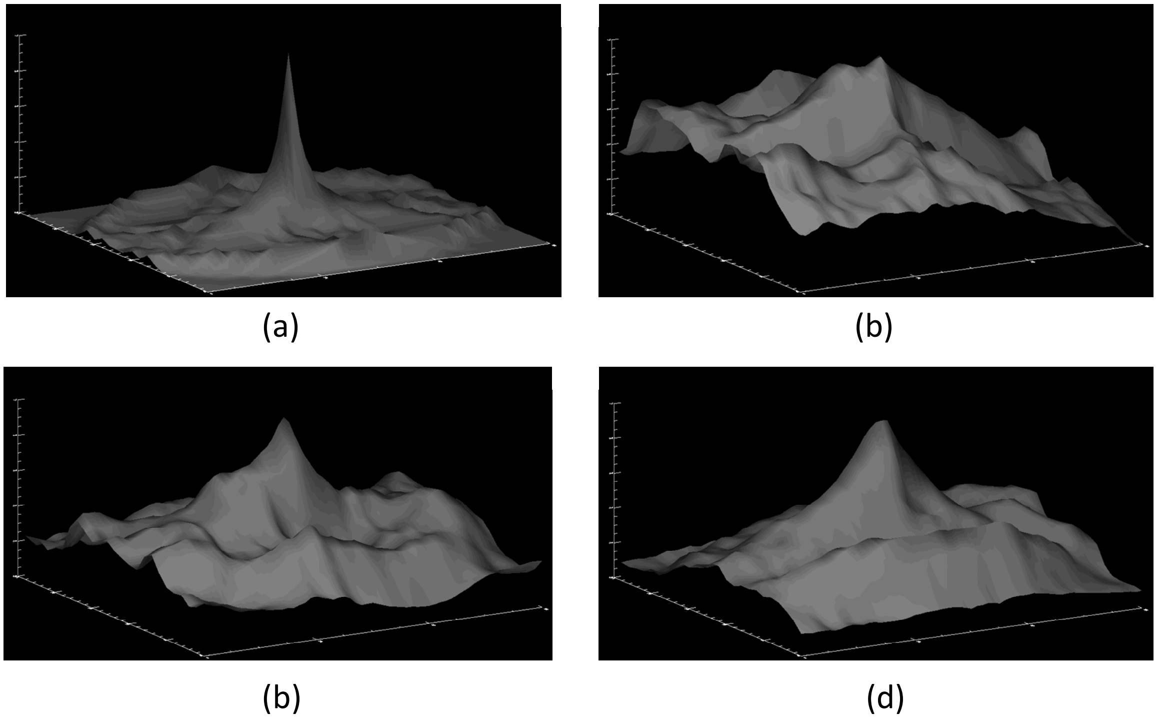

Fig. 5: (a) Segmented self-correlation. (b) First false peak. (c) Second peak a match detected using the standard deviation of the product of inverse self-correlation. (d) Third peak detected by the standard deviation of inverse method.

4. CONCLUSIONS

In this paper, an algorithm for detecting extremely faint fiducials is described. One of the challenges of this real-time algorithm is the extremely low contrast of the fiducial. The other problem is the speed of processing. Currently, we are experimenting with sub-imaging technique to increase the search performance as well reduce the search time. In this work, two different criteria are used to detect a valid match. Shape of the detected correlation is compared to the autocorrelation by using difference or standard deviation of product of inverse of self correlation with the correlation. In addition to these two metrics, other metrics are also being explored [17-18].

ACKNOWLEDGEMENT

This work performed under the auspices of the U.S. Department of Energy by Lawrence Livermore National Laboratory under Contract DE-AC52-07NA27344.

REFERENCES

1. E. I. Moses, "Overview of the National Ignition Facility", *Fusion Science and Technology* **54**, pp. 361-366 (2008).
2. J. V. Candy, W. A. McClay, A. A. S. Awwal, and S. W. Ferguson, "Optimal position estimation for the automatic alignment of a high-energy laser," Journal of Optical Society of America A, Vol. 22, pp. 1348-1356, 2005.
3. R. A. Zacharias, N. R. Beer, E. S. Bliss, et al., "Alignment and wavefront control systems of the National Ignition Facility," Optical Engineering **43**, 2873-2884 (2004).
4. K. Wilhelmsen, A. Awwal, W. Ferguson, B Horowitz, V. Miller Kamm, C. Reynolds, "Automatic Alignment System For The National Ignition Facility", Proceedings of 2007 International Conference on Accelerator and Large Experimental Control Systems (ICALEPCS07), 486-490, Knoxville, Tennessee (2007).
5. A. A. S. Awwal, Wilbert A. McClay, Walter S. Ferguson, James V. Candy, Thad Salmon, and Paul Wegner, "Detection and Tracking of the Back-Reflection of KDP Images in the presence or absence of a Phase mask," Applied Optics, Vol. 45, pp. 3038-3048, May 2006. http://accelconf.web.cern.ch/accelconf/ica07/PAPERS/ROAA02.PDF
6. C. A. Haynam, P. J. Wegner et al., "National Ignition Facility laser performance status," Applied Optics **46**, 3276-3303 (2007).
7. W. A. McClay III, A. A. S. Awwal, S. C. Burkhart, J. V. Candy, "Optimization and improvement of FOA corner cube algorithm," in *Photonic Devices and Algorithms for Computing VI*, edited by K. Iftekharuddin and A. A. S. Awwal, Proc. of SPIE **5556**, 227-232 (2004)
8. A. A. S. Awwal, J. V. Candy, C. A. Haynam, C. C. Widmayer, E. S. Bliss, and S. C. Burkhart, "Accurate Position sensing of defocused beams using simulated beam templates," in *Photonic Devices and Algorithms for Computing VI*, edited by K. Iftekharuddin and A. A. S. Awwal, Proc. of SPIE **5556**, 233-242 (2004).
9. A. A. S. Awwal, "Automatic identification of templates in matched filtering," in *Photonic Devices and Algorithms for Computing VI*, edited by K. Iftekharuddin and A. A. S. Awwal,, Proc. of SPIE **5556**, 102-109 (2004).
10. A. A. S. Awwal, "Multi-object feature detection and error correction for NIF automatic optical alignment" in *Photonic Devices and Algorithms for Computing VIII*, edited by K. Iftekharuddin and A. A. S. Awwal, Proc. SPIE **6310,** 63100Q (2006).
11. A. A. S. Awwal, Kenneth L. Rice, Tarek M. Taha, "Fast implementation of matched-filter-based automatic alignment image processing," Optics & Laser Technology **41**, 193-197 (2009).
12. A. VanderLugt, "Signal Detection by Complex Spatial Filtering", IEEE Trans. Inf. Theory **IT-10**, 139-145 (1964).
13. A. A. S. Awwal, M. A. Karim, and S. R. Jahan, "Improved Correlation Discrimination Using an Amplitude-Modulated Phase-Only Filter," Applied Optics **29**, 233-236 (1990).
14. M. A. Karim and A. A. S. Awwal, *Optical Computing: An Introduction*, John Wiley, New York, NY, 1992.
15. K. M. Iftekharuddin, M. A. Karim, and A. A. S. Awwal, "Optimization of Amplitude Modulated Inverse Filter", Mathematical and Computer Modeling **24**, 103-112 (1996).
16. Karl S. Gudmundsson, and A. A. S. Awwal, "Sub-Imaging Technique to Improve POF Search Capability", Applied Optics **42**, 4709-4717 (2003).
17. B. V. K. Vijay Kumar and L. Hassebrook, "Performance measures for correlation filters," Applied Optics **29,** 2997-3006 (1990).
18. T. Wolf, B. Gutman, H. Weber, J. Ferre-Borrull, S. Bosch, and S. Vallmitjana, "Application of fuzzy-rule-based postprocessing to correlation methods in pattern recognition," Appl. Opt. **35**, 6955-6963, (1996).